Improvement of Ti/Al/Ti Ohmic contacts on AlGaN/GaN heterostructures by insertion of a thin carbon interfacial layer

G. Greco [ID] ; S. Di Franco [ID] ; R. Lo Nigro [ID] ; C. Bongiorno [ID] ; M. Spera; P. Badalà [ID] ; F. Iucolano;
F. Roccaforte [✉] [ID]

Check for updates

View Online

Export Citation

Applied Physics Letters

Articles You May Be Interested In

Schottky contacts on sulfurized silicon carbide (4H-SiC) surface

Appl. Phys. Lett. (March 2024)

Space charge limited current in 4H-SiC Schottky diodes in the presence of stacking faults

Appl. Phys. Lett. (August 2023)

Mechanism of low-temperature-annealed Ohmic contacts to AlGaN/GaN heterostructures: A study via formation and removal of Ta-based Ohmic-metals

Appl. Phys. Lett. (February 2022)

Improvement of Ti/Al/Ti Ohmic contacts on AlGaN/GaN heterostructures by insertion of a thin carbon interfacial layer

View Online   Export Citation   CrossMark

G. Greco,[1] S. Di Franco,[1] R. Lo Nigro,[1] C. Bongiorno,[1] M. Spera,[2] P. Badalà,[2] F. Iucolano,[2] and F. Roccaforte[1,a]

AFFILIATIONS

[1]CNR-IMM, Strada VIII, n. 5 – Zona Industriale, 95121 Catania, Italy
[2]STMicroelectronics, Stradale Primosole 50, 95121 Catania, Italy

[a]Author to whom correspondence should be addressed: fabrizio.roccaforte@imm.cnr.it

ABSTRACT

This Letter reports on the improvement of the morphological and electrical behavior in Ti/Al/Ti Ohmic contacts on AlGaN/GaN heterostructures by the insertion of a thin carbon interfacial layer. In particular, the presence of a carbon layer between the Ti/Al/Ti metal stack and the AlGaN surface leads to the lowering of the annealing temperature (down to 450 °C) required to obtain linear I–V curves and to the improvement of the contacts surface morphology. The temperature dependence of the specific contact resistance was explained by the thermionic field emission, with a reduction in the barrier height Φ_B down to 0.62 eV in the annealed contacts with the interfacial carbon layer. The experimental evidence has been justified with the formation of a thin low work function TiC layer, which enhances the current conduction through the metal/AlGaN interface.

Gallium nitride (GaN) and the related AlGaN/GaN heterostructures are excellent materials for high-power and high-frequency devices.[1] In this context, Ohmic contacts are fundamental bricks for the fabrication of AlGaN/GaN high electron mobility transistors (HEMTs),[2] since a low resistance of source-drain contacts is required to minimize the device on-resistance and power losses of these transistors.

One of the most common approaches to achieve good Ohmic contacts on GaN HEMTs is using annealed Ti/Al/X/Au multilayers (X = Ni, Ti, Pt, Pd, Mo, Re, Ir).[2] In general, the presence of Au in Ti/Al/X/Au multilayer is crucial for the formation of Ohmic contacts. In fact, the formation of low-resistivity Al_2Au and $AlAu_4$ phases in the reacted layer and at the interface provides preferential conductive paths for the current flow through the contact.[3,4] Moreover, the presence of Au is believed to enhance Ga diffusion from the AlGaN surface, thus favoring the formation of TiN at the metal/AlGaN interface.[5] In this way, the TiN formation leaves behind N-vacancies in the AlGaN, which act as donors and makes more efficient the Ohmic contact formation by a tunneling mechanism through the barrier. However, to achieve the compatibility of GaN on Silicon technology with a CMOS industrial environment, "Au-free" metallization are required.[6]

To obtain "Au-free" Ohmic contacts on AlGaN/GaN heterostructures, Ti/Al-based schemes are often adopted, because of the low work function of Ti and Al and of the phases formed upon their mutual reaction occurring upon annealing. However, many parameters can influence the performance of these contacts, such as the annealing conditions,[7,8] the Ti/Al thickness ratio,[2,9] or the heterostructure properties.[2,10] Then, to reduce the dependence of the electrical behavior on the Au-free contact formation parameters, other approaches acting on the underlying semiconductor layer have been explored in the literature, e.g., the selective n-type ion-implantation doping,[11] the regrowth of a highly-doped region,[12,13] or the contact recession by an AlGaN etch.[14,15] However, all these approaches introduce additional processing steps that increase the complexity of the device fabrication flow.

Some authors focused on the importance of the metal layer in intimate contact with the AlGaN semiconductor. Vanko et al.[16] introduced a thin layer of Nb at the interface with the AlGaN to decrease the specific contact resistance of Ti/Al/Ni/Au contacts and reduce their roughness. A similar approach have been pursued by Park et al.,[17] who obtained quasi-linear current–voltage (I–V) curves using non-annealed Cr/graphene contacts. In this case, the introduction of a graphene interlayer between Cr and AlGaN resulted in a local n-type

06 December 2024 08:21:03

doping of the regions below the contacts with the consequent pinning of the Fermi level, which promotes the carrier transport through the AlGaN layer. Later, Fisichella *et al.*[18] observed a reduction in the barrier height from 0.9 to 0.4 eV by inserting a thin graphene layer in Au/AlGaN contacts, thus leading to a shift from Schottky to Ohmic behavior of the contacts. Moreover, the use of graphene has been proposed to achieve Ohmic contact to either n- or p-type GaN.[19] Indeed, wrinkles with zigzag or armchair direction lead to decrease or increase the local work function, moving the local Fermi level toward conduction or valence band.[19] However, the graphene deposition on large area GaN-on-Si wafers is not straightforward and its integration in a HEMT fabrication flow may introduce additional compatibility issues.

In this Letter, we propose the use of a thin carbon layer at the interface between the metal stack and the AlGaN/GaN heterostructure to improve the morphological and electrical behavior of Ti/Al/Ti Ohmic contacts.

The work has been carried out on $Al_{0.26}Ga_{0.74}N$/GaN heterostructures grown on Si, with an AlGaN thickness of 16 nm. CMOS-compatible Ohmic contacts have been fabricated on these samples using a $Ti_{(40 nm)}$/$Al_{(300 nm)}$/$Ti_{(20 nm)}$ with a thin carbon layer ($\sim$5 nm) between the AlGaN/GaN heterostructure and the metal stack deposited by e-beam evaporation in a Evatec BAK SAW 761, operating at a base pressure of 1×10^{-6} mbar.

For the sake of comparison, reference Ti/Al/Ti contacts without the carbon interfacial layer have been also fabricated. Linear transmission line model (TLM) structures have been produced by standard photolithography and lift-off of the metals. The TLM structures consisted of $100 \times 200 \, \mu m^2$ rectangular pads placed at distances d varying between 20 and 100 μm. Rapid thermal annealing (RTA) of the contacts processes have been performed in Ar atmosphere using a Jipelec JetFirst 150 furnace. The current–voltage (I–V) curves were acquired on the TLM structures on a Karl Suss Microtec probe station equipped with a HP 4156B parameter analyzer. The contacts surface morphology was investigated by atomic force microscopy (AFM), using a Veeco Dimension 3100 microscope. Structural characterization of the layer after annealing was carried out by x-ray diffraction (XRD) using a Bruker-AXS D5005 h–h diffractometer. Finally, transmission electron microscopy (TEM) analyses in cross section were performed using a 200 kV JEOL 2010F microscope, equipped with a Gatan imaging filter (GIF) spectrometer allowing electron energy loss spectroscopy (EELS).

The I–V characteristics of Ti/Al/Ti contacts with the carbon interface layer, acquired on TLM patterns at a distance d of 20 μm for different annealing temperatures up to 500 °C, are reported in Fig. 1(a). As one can see, despite the contacts displayed a strongly rectifying behavior up to an annealing temperature of 400 °C, the annealing at 450 °C already results into an Ohmic behavior. Moreover, a further improvement of the electrical characteristics is obtained at the annealing temperature of 500 °C, with an increase in the current of more than a factor of 3. The inset of Fig. 1(a) compares the I–V curves acquired on the TLM patterns (d = 20 μm) of Ti/Al/Ti contacts annealed at 500 °C with and without the carbon interface layer. Evidently, after annealing at 500 °C, a highly rectifying behavior (with an extremely low current) is observed in the reference Ti/Al/Ti contacts without interlayer, compared with the linear I–V curves obtained in the contact with the carbon layer annealed under the same conditions. Then, Fig. 1(b) shows the plot of the total resistance R_{TOT} as a function of the distance d between adjacent TLM pads, measured in the Ti/Al/Ti Ohmic contacts with the C interlayer formed at 500 °C. The corresponding I–V characteristics are displayed in the inset of the same figure. From the TLM analysis, a specific contact resistance $\rho_c = 3.5 \times 10^{-4}$ Ω cm^2 and a sheet resistance $R_{SH} = 683$ Ω/sq were determined. The same Ti/Al/Ti stack without the interfacial carbon layer exhibits an Ohmic behavior only after annealing at higher temperature (600 °C).[6] TLM analysis on such contacts gave a ρ_c value of 2.2×10^{-3} Ω cm^2, i.e., much higher than the value found for the contact with the carbon interfacial layer. This result clearly demonstrates the benefit of the introduction of this layer at the interface before annealing. As a matter of fact, a comparison with the literature typically shows that good Au-free Ohmic contacts are achievable at annealing temperature below 600 °C only in recessed contacts.[8,9,14,15,20]

A further advantage obtained by the introduction of the carbon layer at the interface with the AlGaN is the improvement of the contact morphology. Figure 2 shows the AFM morphology, acquired on a $10 \times 10 \, \mu m^2$ region, of the Ti/Al/Ti contacts annealed at 500 °C, with and without the carbon layer. The surface of the reference Ti/Al/Ti contact without the carbon interfacial layer [Fig. 1(a)] is characterized by flat areas with some large hillocks, which lead to high values of root mean square roughness (RMS). On the other hand, as visible in Fig. 2(b), the insertion of a carbon interfacial layer resulted in an overall smoother surface with RMS values of 10 nm. In this context, it is
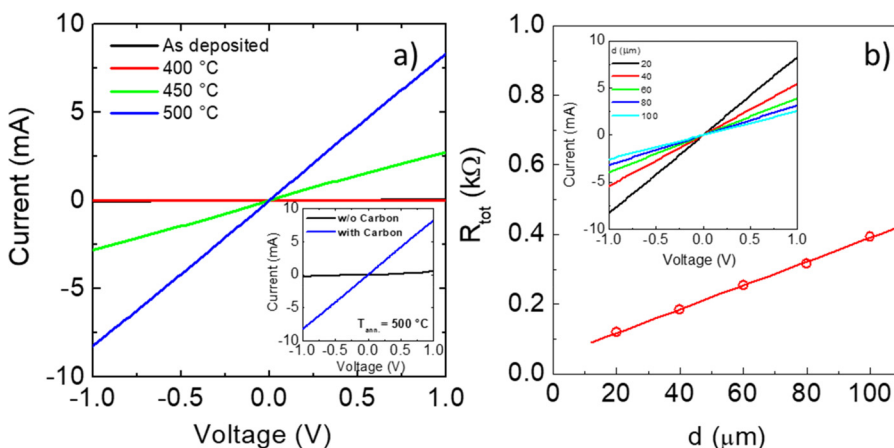
FIG. 1. (a) I–V curves of Ti/Al/Ti contacts with a carbon interfacial layer acquired on TLM patterns at a distance of 20 μm for different annealing temperatures up to 500 °C. The inset shows the comparison between the I–V curves of the contacts annealed at 500 °C with and without the carbon interface layer. (b) Total resistance R_{TOT} as a function of the distance d of adjacent TLM pads of Ti/Al/Ti contacts with a carbon interfacial layer annealed at 500 °C. The inset displays the corresponding I-V characteristics for different TLM distances.

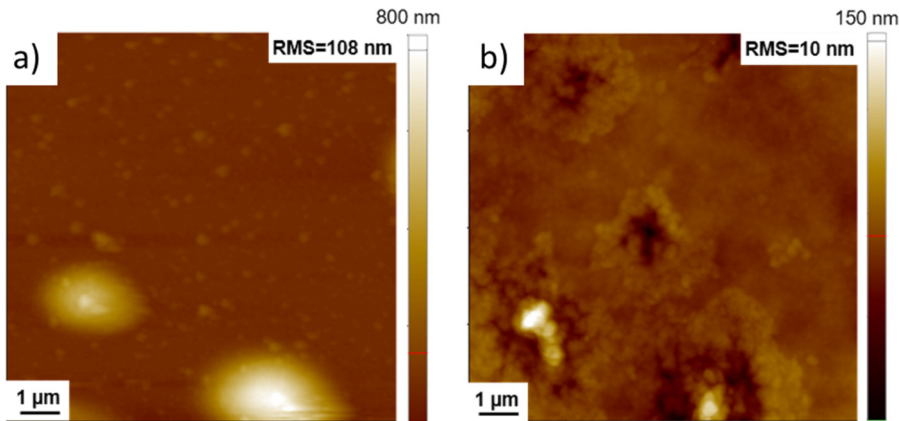**FIG. 2.** AFM images on $10 \times 10\, \mu m^2$ scan areas of Ti/Al/Ti contacts annealed at 500 °C without (a) and with (b) the carbon interfacial layer.

known that Ti–Al based contacts are susceptible to strong reactions with the underlying AlGaN layer upon high-temperature annealing, thus resulting in rough contact surfaces with the possible formation of pronounced hillocks.[21,22] This behavior is often attributed to the low Al melting point (about 660 °C).[20,23] In the presence of Au layer, the higher annealing temperature necessary for Ohmic contact formation (about 800 °C) and the formation of Al_2Au or $AlAu_4$ phases are typically indicated as the causes of the high surface roughness.[3,24,25] However, in Au-free contacts, where the annealing temperature is reduced at around 600 °C, the formation of hillocks and the consequent increase in the RMS are also often observed.[21,26] The hillocks' generation has been correlated with the necessity to relieve the stress created by the different thermal expansion coefficients between the metal film and substrate.[26] Hence, we argue that the presence of the thin carbon layer at the interface between the metal and the AlGaN mitigates this effect, improving the contacts' surface morphology. A similar justification has been given by Vanko *et al.*[16] to explain the behavior of Ti/Al/Ni/Au contacts with a Nb interfacial layer.

XRD analyses have been carried out to monitor the formation of new phases in the annealed Ti/Al/Ti contacts with and without the Carbon interfacial layer. As can be seen in Fig. 3, no differences in the XRD spectra could be observed between the two samples using this technique. In fact, in both cases, the dominant phase is represented by the Al_3Ti, as typically occurs in Ti/Al based contacts,[7,27] with the coexistence of the Al_5Ti_2 phase and some unreacted Al.[28]

In order to acquire additional information on the microstructure of the Ti/Al/Ti contacts with the carbon interfacial layer, TEM analysis has been performed on the sample annealed at 500 °C. Figure 4(a) shows the low magnification bright field TEM micrograph of the sample acquired in the interface region. These analyses confirm the formation of Al–Ti phases, which are predominant inside the reacted contact, while a darker layer is observed at interface with the AlGaN. Figure 4(b) shows the metal/AlGaN interface at higher magnification. As can be seen, the layer formed during reaction is preferentially aligned with the underlying AlGaN and has a thickness of 2.5 nm layer, which in some regions reaches 5 nm. Electron energy loss spectroscopy (EELS) analyses [see Fig. 4(c)] were used to identify the nature of this layer, clearly displaying the peaks corresponding to Ti and C close to the AlGaN surface, in agreement with the presence of the thin TiC layer aligned with the underlying AlGaN.

Also in other wide bandgap semiconductor as silicon carbide (SiC), the presence of a TiC interfacial layer, formed by the reaction between the Ti and the SiC below, leads to Ohmic contact formation with a low specific contact resistance.[29,30]

In AlGaN/GaN heterostructures, the Ohmic contact formation is often correlated with the presence of TiN formed at the metal/AlGaN interface.[21,31] In particular, the reactions leading to the formation of TiN is accompanied by the generation of nitrogen vacancies in the semiconductor, having a donor-like behavior that favors the formation of a tunneling Ohmic contact.[2,4] However, in our case, the low annealing temperature of 500 °C does not allow the formation of the TiN phase at the metal/AlGaN interface, as reported elsewhere.[21,24] Other works, attribute the Ohmic contact formation to the intermixing of the metallic multilayers and the formation of low work function phases at the interface with the AlGaN.[32] In particular, Geneen *et al.*[33] indicated the consuming of the Ti layer at the interface and the formation of epitaxial or aligned metal layer at the interface the key factor to achieve
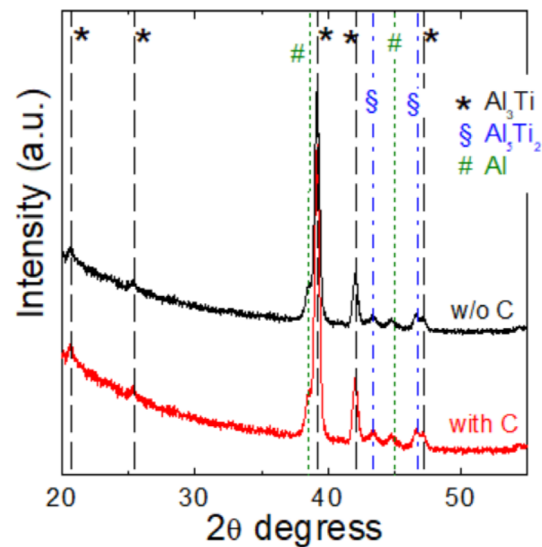

FIG. 3. XRD patterns for Ti/Al/Ti contacts annealed at 500 °C without (black line) and with (red line) the carbon interfacial layer.

FIG. 5. Temperature dependence of specific contact resistance ρ_c for Ti/Al/Ti contacts without ($T_{ann.} = 600\,°C$) and with ($T_{ann.} = 500\,°C$) the carbon interfacial layer. The continuous lines represent the TFE fit of the experimental data. The inset shows a schematic band diagram in the two cases.
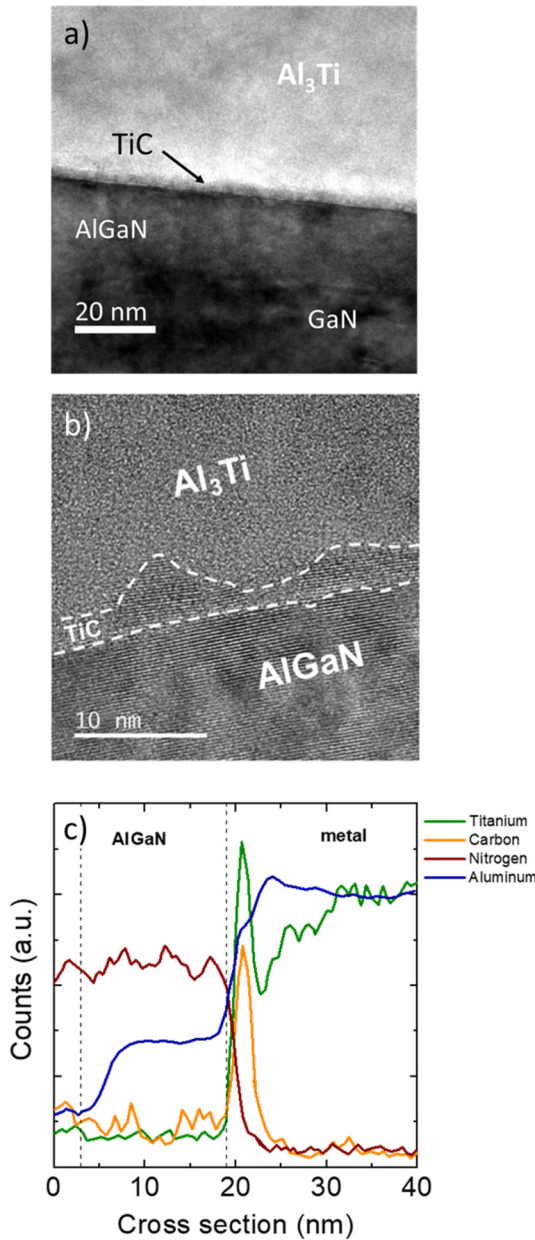

FIG. 4. Cross-sectional low (a) and high (b) magnification TEM micrographs and corresponding EELS analysis (c) acquired at the interface of Ti/Al/Ti contacts with a carbon interfacial layer subjected to an annealing at 500 °C.

low specific contact Ohmic contact. In our present study, it is possible to argue that the formation of the TiC interface layer aligned to the underlying AlGaN layer, having a low work function,[34] is the responsible for the Ohmic contacts formation.

The carrier transport through the metal/semiconductor interface was studied in more detail by I–V measurements on TLM structures as a function o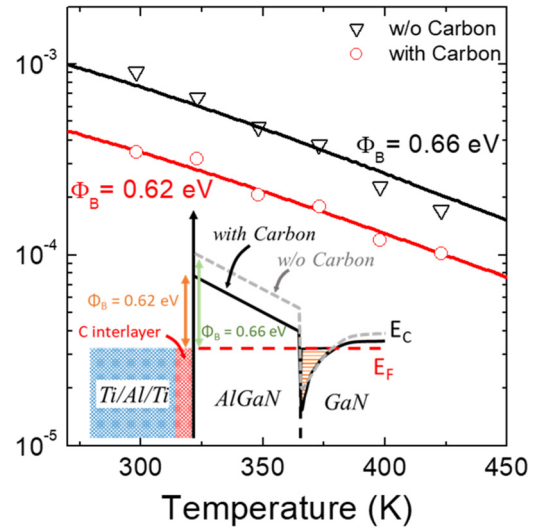f the temperature. Figure 5 reports the values of the specific contact resistance ρ_c, extracted by TLM analysis, as a function of the measurement temperature T for the Ti/Al/Ti contact without and with the C interfacial layer. The values of ρ_c in the two contacts decreases with increasing the measurement temperature. In both cases, the temperature behavior of ρ_c could be well fitted (continuous line) by the thermionic field emission (TFE) model[35] according to the following equation:

$$\rho_c = \left(\frac{1}{qA^*}\right) \frac{k^2}{\sqrt{\pi(\Phi_B + V_n)E_{00}}} \cosh\left(\frac{E_{00}}{kT}\right) \times \sqrt{\coth\left(\frac{E_{00}}{kT}\right)}$$
$$\times \exp\left(\frac{\Phi_B + V_n}{E_{00}\coth\left(\frac{E_{00}}{kT}\right)} - \frac{V_n}{kT}\right), \tag{1}$$

where q is the elementary charge, k is the Boltzmann constant, T is the absolute temperature, A^* is the Richardson constant, V_n is the energy difference between the conduction-band edge and the Fermi level, and E_{00} is the characteristic energy, which quantifies the tunneling component of the current transport.[35]

In our case, an $E_{00} = 47\,meV$ was extrapolated by the fit of the experimental data for both contacts, i.e., for sample with and without carbon interface layer.

In the classical description of doped semiconductor, the characteristics energy E_{00} describing the TFE model depends on the doping concentration of the semiconductor N_D. However, in AlGaN/GaN heterostructures, the term N_D can be replaced with the term N_{D-2DEG} to take into account the sheet carrier density of the 2DEG (n_S) and the distance between the 2DEG and the metal/AlGaN interface, which can be approximated with the thickness of the AlGaN barrier layer (d_{AlGaN}). Then, in the case of heterostructure, the characteristic energy can be defined as[2,10]

$$E_{00} = \frac{h}{4\pi}\sqrt{\frac{N_{D-2DEG}}{m^*\varepsilon_0\varepsilon_{AlGaN}}} \approx \frac{h}{4\pi}\sqrt{\frac{n_S}{m^*\varepsilon_0\varepsilon_{AlGaN}\ d_{AlGaN}}}, \qquad (2)$$

where h is the Planck constant, ε_0 is the dielectric vacuum permittivity, ε_{AlGaN} is the dielectric permittivity for AlGaN, and m^* is the effective mass for electron in AlGaN.

Then, by considering Eq. (2), a sheet carrier density of n_S $\sim 2 \times 10^{13}$ cm^{-2} was obtained in the two cases, which is in agreement with the theoretical value estimated by the *Ambacher*'s model for an AlGaN/GaN heterostructures with these properties (i.e., an Al concentration of the 25% and an AlGaN thickness of 16 nm).[36] Instead, Schottky barrier height values of $\Phi_B = 0.66$ and 0.62 eV were estimated in the case of sample without and with C interface layer, respectively. The lower Φ_B measured in the contact with the carbon interfacial layer is coherent with the reduced ρ_c values. Hence, the presence of the TiC layer at the metal/AlGaN interface can be considered the origin of the lower extrapolated Φ_B and of the improvement of the contact properties. This situation is illustrated in the inset of Fig. 5, reporting a schematic band diagram of the system in the two cases.

In conclusion, the improvement of the morphological and electrical properties of Au-free Ti/Al/Ti Ohmic contacts on AlGaN/GaN heterostructures by the insertion of an interfacial carbon layer was presented and discussed in this Letter. The introduction of the carbon interfacial layer produced beneficial effects under the morphological and electrical point of view. Indeed, it was possible to reduce the annealing temperature needed for the Ohmic contact formation down to 450 °C. In particular, in the presence of the carbon interfacial layer, the annealed Ti/AlTi Ohmic contacts exhibited a much smoother surface and a lower specific contact resistance of 3.5×10^{-4} Ω cm^2. The carrier transport mechanism has been investigated by monitoring temperature dependence of ρ_c, which was explained by the TFE model with a barrier height of 0.62 eV. A microstructural and chemical analysis of the interface enabled to demonstrate the formation of a TiC layer at the interface, preferentially aligned with the underlying AlGaN, which can be responsible for the overall improvement of the contact's properties.

The results can be useful for establishing new routes for Au-free Ohmic contacts for GaN-on-Si HEMT technology.

AUTHOR DECLARATIONS
Conflict of Interest

The authors have no conflicts to disclose.

Author Contributions

Giuseppe Greco: Conceptualization (equal); Data curation (lead); Formal analysis (lead); Writing – original draft (lead). **Salvatore Di Franco:** Investigation (equal). **Raffaella Lo Nigro:** Data curation (equal); Formal analysis (equal). **Corrado Bongiorno:** Investigation (equal). **Monia Spera:** Investigation (equal). **paolo badalà:** Investigation (equal). **Ferdinando Iucolano:** Conceptualization (supporting); Validation (equal). **Fabrizio Roccaforte:** Conceptualization (equal); Data curation (equal); Formal analysis (equal); Funding acquisition (equal); Supervision (equal); Validation (equal); Writing – review & editing (equal).

DATA AVAILABILITY

The data that support the findings of this study are availablefrom the corresponding author upon reasonable request.

REFERENCES

[1] F. Roccaforte, P. Fiorenza, R. Lo Nigro, F. Giannazzo, and G. Greco, "Physics and technology of gallium nitride materials for power electronics," Riv. Nuovo Cimento **41**, 625–681 (2018).

[2] G. Greco, F. Iucolano, and F. Roccaforte, Appl. Surf. Sci. **383**, 324 (2016).

[3] F. Roccaforte, F. Iucolano, F. Giannazzo, A. Alberti, and V. Raineri, Appl. Phys. Lett. **89**, 022103 (2006).

[4] F. Iucolano, G. Greco, and F. Roccaforte, Appl. Phys. Lett. **103**, 201604 (2013).

[5] A. Shriki, R. Winter, Y. Calahorra, Y. Kauffmann, G. Ankonina, M. Eizenberg, and D. Ritter, J. Appl. Phys. **121**, 065301 (2017).

[6] F. Roccaforte, P. Fiorenza, G. Greco, R. Lo Nigro, F. Giannazzo, F. Iucolano, and M. Saggio, Microelectron. Eng. **187–188**, 66–77 (2018).

[7] G. Greco, F. Giannazzo, F. Iucolano, R. Lo Nigro, and F. Roccaforte, J. Appl. Phys. **114**, 083717 (2013).

[8] A. Firrincieli, B. De Jaeger, S. You, D. Wellekens, M. V. Hove, and S. Decoutere, Jpn. J. Appl. Phys., Part 1 **53**, 04EF01 (2014).

[9] T. Yoshida and T. Egawa, Semicond. Sci. Technol. **33**, 075006 (2018).

[10] A. Constant, E. Claeys, J. Baele, P. Coppens, and F. D. Pestel, Mater. Sci. Semicond. Process. **129**, 105806 (2021).

[11] F. Roccaforte, F. Giannazzo, and G. Greco, Micro **2**, 23–53 (2022).

[12] H.-C. Seo, P. Chapman, H.-I. Cho, J.-H. Lee, and K. K. Kim, Appl. Phys. Lett. **93**, 102102 (2008).

[13] W. Wojtasiak, M. Góralczyk, D. Gryglewski, M. Zając, R. Kucharski, P. Prystawko, A. Piotrowska, M. Ekielski, E. Kamińska, A. Taube, and M. Wzorek, Micromachines **9**, 546 (2018).

[14] H.-S. Lee, D. S. Lee, and T. Palacios, IEEE Electron Device Lett. **32**, 623 (2011).

[15] T. Yoshida and T. Egawa, Jpn. J. Appl. Phys., Part 1 **57**, 110302 (2018).

[16] G. Vanko, T. Lalinsky, Z. Mozolova, J. Liday, P. Vogrincic, A. Vincze, F. Uherek, S. Hascík, and I. Kostic, Vacuum **82**, 193–196 (2007).

[17] P. Sung Park, K. M. Reddy, D. N. Nath, Z. Yang, N. P. Padture, and S. Rajan, Appl. Phys. Lett. **102**, 153501 (2013).

[18] G. Fisichella, G. Greco, F. Roccaforte, and F. Giannazzo, Appl. Phys. Lett. **105**, 063117 (2014).

[19] H. Zhong, Z. Liu, L. Shi, G. Xu, Y. Fan, Z. Huang, J. Wang, G. Ren, and K. Xu, Appl. Phys. Lett. **104**, 212101 (2014).

[20] R. Gong, J. Wang, S. Liu, Z. Dong, M. Yu, C. P. Wen, Y. Cai, and B. Zhang, Appl. Phys. Lett. **97**, 062115 (2010).

[21] M. Spera, G. Greco, R. Lo Nigro, S. Scalese, C. Bongiorno, M. Cannas, F. Giannazzo, and F. Roccaforte, Energies **12**, 2655 (2019).

[22] N. Chaturvedi, U. Zeimer, J. Würfl, and G. Trankle, Semicond. Sci. Technol. **21**, 175–179 (2006).

[23] S. S. Mahajan, A. Dhaul, R. Laishramm, S. Kapoor, S. Vinayak, and B. K. Sehgal, Mater. Sci. Eng. B **183**, 47 (2014).

[24] A. N. Bright, P. J. Thomas, M. Weyland, D. M. Tricker, C. J. Humphreys, and R. Davies, J. Appl. Phys. **89**, 3143 (2001).

[25] D. Selvanathan, F. M. Mohammed, A. Tesfayesus, and I. Adesida, J. Vac. Sci. Technol. B **22**, 2409 (2004).

[26] J. S. Kwak, S. E. Mohney, J. Y. Lin, and R. S. Kern, Semicond. Sci. Technol. **15**, 756–760 (2000).

[27] G. Greco, F. Iucolano, C. Bongiorno, F. Giannazzo, M. Krysko, M. Leszczynski, and F. Roccaforte, Appl. Surf. Sci. **314**, 546–551 (2014).

[28] A. Constant, J. Baele, P. Coppens, W. Qin, H. Ziad, E. De Backer, P. Moens, and M. Tack, J. Appl. Phys. **120**, 104502 (2016).

[29] M. Vivona, G. Greco, C. Bongiorno, R. Lo Nigro, S. Scalese, and F. Roccaforte, Appl. Surf. Sci. **420**, 331–335 (2017).

06 December 2024 08:21:03

[30]M. Vivona, G. Greco, R. Lo Nigro, C. Bongiorno, and F. Roccaforte, J. Appl. Phys. **118**(3), 035705 (2015).

[31]J. Zhang, X. Kang, X. Wang, S. Huang, C. Chen, K. Wei, Y. Zheng, Q. Zhou, W. Chen, B. Zhang, and X. Liu, IEEE Electron Device Lett. **39**, 847 (2018).

[32]Y. Li, G. I. Ng, S. Arulkumaran, C. M. M. Kumar, K. S. Ang, M. J. Anand, H. Wang, R. Hofstetter, and G. Ye, Appl. Phys. Express **6**, 116501 (2013).

[33]F. Geenen, A. Constant, E. Solano, D. Deduytsche, C. Mocuta, P. Coppens, and C. Detavernier, J. Appl. Phys. **127**, 215701 (2020).

[34]H. Zhu, M. Aindow, and R. Ramprasad, Phys. Rev. B **80**, 201406 (2009).

[35]F. A. Padovani and R. Stratton, Solid-State Electron. **9**, 695–707 (1966).

[36]O. Ambacher, J. Smart, J. R. Shealy, N. G. Weimann, K. Chu, M. Murphy, W. J. Schaff, and L. F. Eastman, J. Appl. Phys. **85**, 3222 (1999).

06 December 2024 08:21:03